Molecular orbital projectors in non-empirical jmDFT recover exact conditions in transition-metal chemistry

The Journal of Chemical Physics

Molecular orbital projectors in non-empirical jmDFT recover exact conditions in transition-metal chemistry

Cite as: J. Chem. Phys. **156**, 184112 (2022); https://doi.org/10.1063/5.0089460
Submitted: 25 February 2022 • Accepted: 20 April 2022 • Accepted Manuscript Online: 21 April 2022 • Published Online: 11 May 2022

Published open access through an agreement with Massachusetts Institute of Technology

Akash Bajaj, Chenru Duan, Aditya Nandy, et al.

The Journal of Chemical Physics ARTICLE scitation.org/journal/jcp

Molecular orbital projectors in non-empirical jmDFT recover exact conditions in transition-metal chemistry

Cite as: J. Chem. Phys. 156, 184112 (2022); doi: 10.1063/5.0089460
Submitted: 25 February 2022 • Accepted: 20 April 2022 •
Published Online: 11 May 2022

Akash Bajaj,[1,2] Chenru Duan,[1,3] Aditya Nandy,[1,3] Michael G. Taylor,[1] and Heather J. Kulik[1,a)]

AFFILIATIONS

[1] Department of Chemical Engineering, Massachusetts Institute of Technology, Cambridge, Massachusetts 02139, USA
[2] Department of Materials Science and Engineering, Massachusetts Institute of Technology, Cambridge, Massachusetts 02139, USA
[3] Department of Chemistry, Massachusetts Institute of Technology, Cambridge, Massachusetts 02139, USA

[a)] **Author to whom correspondence should be addressed:** hjkulik@mit.edu. **Tel.:** 617-253-4584

ABSTRACT

Low-cost, non-empirical corrections to semi-local density functional theory are essential for accurately modeling transition-metal chemistry. Here, we demonstrate the judiciously modified density functional theory (jmDFT) approach with non-empirical U and J parameters obtained directly from frontier orbital energetics on a series of transition-metal complexes. We curate a set of nine representative Ti(III) and V(IV) d^1 transition-metal complexes and evaluate their flat-plane errors along the fractional spin and charge lines. We demonstrate that while jmDFT improves upon both DFT+U and semi-local DFT with the standard atomic orbital projectors (AOPs), it does so inefficiently. We rationalize these inefficiencies by quantifying hybridization in the relevant frontier orbitals. To overcome these limitations, we introduce a procedure for computing a molecular orbital projector (MOP) basis for use with jmDFT. We demonstrate this single set of d^1 MOPs to be suitable for nearly eliminating all energetic delocalization and static correlation errors. In all cases, MOP jmDFT outperforms AOP jmDFT, and it eliminates most flat-plane errors at non-empirical values. Unlike DFT+U or hybrid functionals, jmDFT nearly eliminates energetic delocalization and static correlation errors within a non-empirical framework.

I. INTRODUCTION

Applied Kohn–Sham density functional theory (DFT)[1–4] is widely employed in transition-metal chemistry due to its good balance of cost and accuracy.[5,6] However, common local[7,8] and semi-local[9–11] approximations to the exchange–correlation (xc) functional within DFT exhibit one- and many-electron self-interaction errors (SIEs), also referred to as the delocalization error (DE).[12–16] These errors can be traced back to the fact that these approximations lack key properties of the exact functional, including a derivative discontinuity and piecewise linearity upon fractional charge addition.[17–23] These DEs[24–27] are associated with erroneous predictions of densities,[24,28–32] electron affinities,[33–36] band gaps,[27,37,38] spin-state ordering,[39–47] and other properties.[48–51] Among the possible generalizations[52,53] to Kohn–Sham DFT that help mitigate these errors,[51,54–66] the DFT+U approach[67–71] is commonly employed for transition-metal-containing systems[39,72–83] as it allows a targeted accounting of electronic correlation of the localized electrons (i.e., d or f) at the cost of semi-local DFT.[70]

The simplified,[69,71] rotationally invariant[68] form of DFT+U is

$$E^{\mathrm{DFT+U}} = E^{\mathrm{DFT}} + \frac{1}{2}\sum_{I,\sigma}\sum_{nl} U^I_{nl}\left[\mathrm{Tr}\left(\mathbf{n}^{I\sigma}_{nl}\left(\mathbf{1}-\mathbf{n}^{I\sigma}_{nl}\right)\right)\right], \quad (1)$$

where a +U correction is applied on every nl subshell and spin σ on atom I. The occupation matrix $\mathbf{n}^{I\sigma}_{nl}$ is obtained by projecting states $|\psi_{k,v}\rangle$ onto localized atomic orbitals (AOs) from the nl subshell with angular momenta m $|\phi^I_m\rangle$ on site I using

$$n^{I\sigma}_{mm'} = \sum_{k,v}\langle\psi_{k,v}|\phi^I_{m'}\rangle\langle\phi^I_m|\psi_{k,v}\rangle. \quad (2)$$

The deviation from linearity of the energy[17] [i.e., the energetic delocalization error (EDE[28])] is approximately quadratic for most xc functionals.[18,84] Thus, the first-principles motivation for using DFT+U to correct semi-local DFT errors is made clear by the fact that the quadratic DFT+U expression in Eq. (1) should recover piecewise linearity.[71] The only caveat to this analysis is that we require the fractional electron addition to be captured by the projection onto AOs in $\mathbf{n}_{nl}^{I\sigma}$.[84] For the simplified case where electron addition produces quadratic energy dependence and is localized to a single element of the occupation matrix, the U value that recovers piecewise linearity[84–86] is the constant energetic curvature[84] of the original xc functional.

The standard DFT+U approach[67,69,71,87] applied on the metal-centered d AOs of transition-metal (TM) complexes is known to reduce their EDE, albeit at rates lower than the maximum 0.125 eV/eV expected at the atomic limit.[84,88] Moreover, DFT+U can eliminate the EDE entirely at the non-empirically determined U (i.e., the global curvature[18,84]),

$$U = \left\langle \frac{\partial^2 E}{\partial q^2} \right\rangle = \varepsilon_{N+1}^{\mathrm{HOMO}} - \varepsilon_{N}^{\mathrm{LUMO}}, \tag{3}$$

where the global curvature can be suitably approximated to be constant and estimated as the difference in the N+1-electron highest occupied molecular orbital (HOMO) and N-electron lowest unoccupied molecular orbital (LUMO) eigenvalues along the fractional charge line (FCL). Standard DFT+U can fail completely and have no effect on EDE for pathological cases,[84,89] which typically have strong or variable hybridization of AOs to form molecular orbitals (MOs). To overcome these limitations, we introduced[88] a simple scheme for obtaining molecular orbital projectors (MOPs) in DFT+U to eliminate EDE at non-empirical U values. Similar approaches have been useful in the solid state.[90,91] Nevertheless, DFT+U worsens the static correlation error (SCE) for all systems.[85] Methods prone to large SCE, such as Hartree–Fock theory and hybrid functionals,[29] introduce errors that lead to erroneous barrier heights[92,93] and reaction energetics,[94] and fail to adequately describe delocalized ground states (e.g., metallic[95] or conjugated[96] systems). Given the reliance of many high-throughput screening workflows on DFT+U to improve properties without increasing cost,[97] a robust low-cost alternative is needed.

Toward this end, we introduced[85,86] the judiciously modified DFT (jmDFT) approach, wherein the shape of the errors can be fit to any analytical function and then inverted to correct errors along the flat plane. A similar idea has been recently demonstrated with deep learning.[98] The approach also bears some similarities to local orbital scaling corrections.[99,100] The jmDFT approach with atomic projections has been shown as one path to eliminate EDE and SCE simultaneously for isolated atoms and diatomics,[85]

$$\begin{aligned} E^{\mathrm{DFT+U+J}} = E^{\mathrm{DFT}} &+ \frac{1}{2}\sum_{I,\sigma}\sum_{nl}(U_{nl}^{I} - J_{nl}^{I}) \\ &\times \left[\mathrm{Tr}\left(\mathbf{n}_{nl}^{I,\sigma}\left(\mathbf{1} - \mathbf{n}_{nl}^{I,\sigma}\right)\right)\right] \\ &+ \frac{1}{2}\sum_{I,\sigma}\sum_{nl}J_{nl}^{I}\left[\mathrm{Tr}\left(\mathbf{n}_{nl}^{I,\sigma}\mathbf{n}_{nl}^{I,-\sigma}\right)\right], \end{aligned} \tag{4}$$

where the first two terms in this equation correspond to Eq. (1) except that U has been replaced by U-J. The J term alone is insufficient to eliminate energetic errors across the full flat plane due to its monotonic dependence on electron count.[85] For s-electron valences, we introduced a modified J (i.e., J') term,

$$E^{J'} = \frac{1}{2}\sum_{I,\sigma}\sum_{nl}J'^{I}_{nl}\left[\mathrm{Tr}\left(\left(\mathbf{n}_{nl}^{I,\sigma} - 1\right)\left(\mathbf{n}_{nl}^{I,-\sigma} - 1\right)\right)\right]. \tag{5}$$

The coefficients can all be determined non-empirically[86] by extracting the parameter values (i.e., for U, J, or J') from the result of a DFT calculation needing correction. In this case, the U for jmDFT is obtained using the global curvature estimate of Eq. (3). The J (or J') is obtained using $U + J \sim \varepsilon_{N+1}^{\mathrm{HOMO}} - \varepsilon_{N+1}^{\mathrm{LUMO}}$, where the N+1-electron system corresponds to one endpoint of the seam along the flat plane. However, the suitability of this jmDFT approach with standard atomic projections on the EDE and SCE of TM complexes has not been demonstrated.

The exact flat-plane constraint[101] corresponds to two conditions: (i) piecewise linearity of energies as electrons get added from a singlet N−1-electron system to another singlet N+1-electron system passing through the N-electron doublet configuration and (ii) equivalence of the energy for all cases where charge is held constant but the spin of the electron changes (supplementary material, Figure S1). Within TM complexes, a straightforward case where electron addition leads from a singlet to a doublet state is when the metal center has formal d^0 and d^1 configurations, respectively,

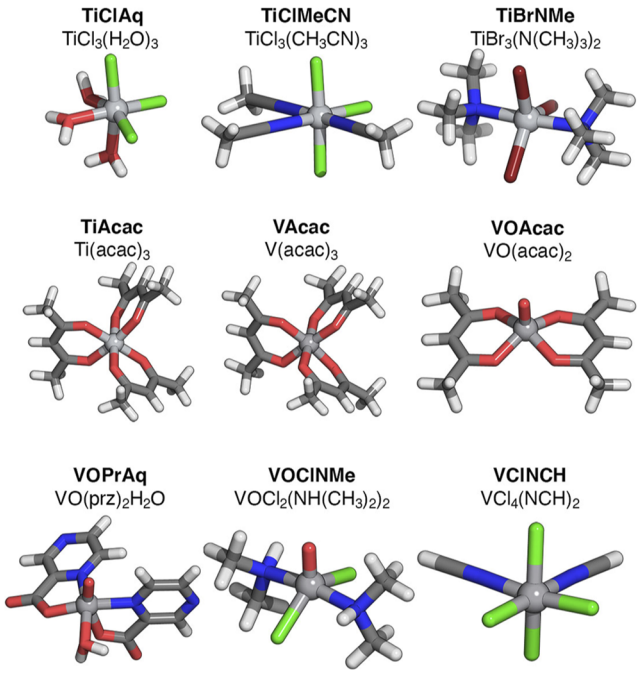

FIG. 1. DFT-optimized structures of Ti and V mononuclear complexes used for flat-plane error analysis. The chemical formula of each structure is annotated, and the nomenclature used for referencing each structure throughout this work is indicated in bold at the top of each structure. Metal centers are shown as silver spheres, whereas hydrogen, carbon, nitrogen, oxygen, chlorine, and bromine atoms are shown in white, gray, blue, red, green, and brown, respectively.

at the atomic limit. Thus, in this work, we investigate the suitability of both standard (i.e., AOP) and molecular (i.e., MOP) jmDFT with non-empirical coefficients to remove flat-plane errors for d^1 Ti(III) and V(IV) complexes (Fig. 1 and supplementary material, Text S1 and Table S1, also see Sec. II). We demonstrate that jmDFT never worsens the static correlation error while improving the delocalization error and that the MOP approach is essential for capturing the degree of hybridization present in the frontier orbitals of these complexes.

II. COMPUTATIONAL DETAILS

We obtained all mononuclear Ti/V transition-metal (TM) complexes with a formal d^1 electron configuration using the Cambridge Structural Database (CSD)[102] v5.41 (with August 2020 update). From a total of 377 initial candidate structures, we selected 50 representative Ti(III) and V(IV) TM complexes, along with an additional $V(acac)_3$ complex in the +3 oxidation state, after validating their user-assigned metal oxidation state (supplementary material, Text S1). Geometry optimizations of all 51 structures were carried out using TeraChem[103] v1.9 using the hybrid generalized gradient approximation (GGA)[11] PBE0 exchange–correlation (xc) functional[104,105] and the LACVP* composite basis set, which consists of an LANL2DZ effective core potential[106,107] for transition metals, Br, and I, and the 6-31G* basis[108] for all other atoms. We confirmed that this choice of a modest basis set for the geometry optimization did not significantly alter conclusions from the plane-wave calculations used to establish and correct flat plane errors (supplementary material, Table S2).

Geometry optimizations were carried out in translation rotation internal coordinates[109] using the L-BFGS algorithm[110–115] with default thresholds of 4.5×10^{-4} hartree/bohr for the gradient and 1×10^{-6} hartree for changes in the self-consistent field (SCF) energy. From these optimized structures, we first selected seven representative cases that were validated to have high fidelity (i.e., root mean squared deviation, i.e., RMSD <0.4 Å) with the CSD structure (supplementary material, Table S1). Two additional Ti complexes [i.e., $TiCl_3(H_2O)_3$ and $TiCl_3(CH_3CN)_3$] required separate optimizations with an implicitly modeled solvent using the conductor-like polarizable continuum model (C-PCM),[116,117] as implemented in TeraChem,[118,119] to satisfy the RMSD criteria. A dielectric of 10 to mimic the crystal field and defaults of 1.2× Bondi's van der Waals radii[120] were used to construct the cavity in thiese cases.

Spin-polarized DFT calculations on these nine optimized structures were carried out with the plane-wave periodic boundary condition code Quantum ESPRESSO[121] v5.1 using the PBE semi-local GGA[11] xc functional. Ultrasoft pseudopotentials[122,123] were employed throughout as obtained from the Quantum-ESPRESSO website with semi-core 3*s* and 3*p* states in the valence for Ti and V (supplementary material, Table S3). Plane-wave cutoffs were selected to be 30 Ry for the wavefunction and 300 Ry for the charge density, as in our prior work on similar systems.[84] All complexes were placed with the metal in the center of a 26.5 Å cubic box to ensure sufficient vacuum, and the Martyna–Tuckerman scheme[124] was employed to eliminate periodic image effects. All optimized and re-centered geometries are provided in the supplementary material zip file. At least 6 and up to a maximum of 14 unoccupied states (i.e., bands) were included for all calculations. To improve SCF convergence, the mixing factor was reduced to 0.4 from its default value, and the convergence threshold for the SCF energy error was loosened to 9×10^{-6} Ry.

All fractional charge calculations were carried out as single-point SCF calculations on the optimized geometries of each TM complex. Fractional electron single-point calculations were carried out while varying the net charge such that the formal metal oxidation state varied from +4 to +3 for Ti and +5 to +4 for V. All fractional electron calculations were carried out in increments of 0.1 e^- by manually altering the band occupations using the "from_input" command in Quantum ESPRESSO.

Plane-wave eigenstates were transformed to their corresponding real-space Wannier function[125] localized molecular orbitals (MOs) using the pmw.x utility available with the Quantum-ESPRESSO package (supplementary material, Text S2). Five contiguous eigenstates were selected using the reduced state of each complex, and their range was specified using the "first_band" and "last_band" keywords (supplementary material, Table S1 and Text S2). To choose the starting index (i.e., the "first_band" value), we selected the band for which the electron would be added or removed (i.e., the majority-spin HOMO) along with four majority-spin bands that were immediately higher in energy. The band numbers depended on the number of atoms as well as the valence states included in the pseudopotentials for each atom type (supplementary material, Tables S1 and S3). Density isosurfaces of molecular orbitals were plotted at ±0.002 e/bohr^3 using the pp.x utility of Quantum ESPRESSO and visualized using the VMD visualization program[126] and VESTA[127] v3.3.9.

III. RESULTS AND DISCUSSION

A. Assessing the reduction of flat-plane errors in transition-metal complexes with standard jmDFT

To determine the suitability of jmDFT as a low-cost method for eliminating both EDE and SCE in molecular systems, we curated a test set of mononuclear octahedral TM complexes (see Sec. II). We start by using jmDFT in its standard form with atomic projectors and assessing how well it reduces both EDE and SCE for nine representative Ti(III) and V(IV) complexes (Fig. 1 and supplementary material, Text S1 and Table S1, and see Sec. II).

We quantify the approximate EDE as the energetic deviation ($E^{dev.}$) from linearity that occurs at the midpoint of the d^0 to d^1 FCL, as in prior work[84] (Fig. 2 and supplementary material, Fig. S1). Because constant average curvature is common, the assumption that the energetic deviation is maximum at the midpoint holds well in most cases. We can estimate the maximum deviation using the frontier eigenvalues of the d^0 (i.e., N-electron) and d^1 (i.e., $N+1$-electron) systems,[18,26,84]

$$E^{dev.} = \frac{\varepsilon_N^{LUMO} - \varepsilon_{N+1}^{HOMO}}{8}. \quad (6)$$

Because the +U correction is a key component in the jmDFT expressions, we expect jmDFT to reduce the EDE for our Ti and V complexes. Indeed, using the non-empirical jmDFT U and J on the metal d atomic projections always leads to a smaller magnitude of $E^{dev.}$ (<0.5 eV) relative to the 0.5–0.7 eV EDE obtained with semi-local DFT (i.e., PBE,[11] Fig. 2 and supplementary material, Tables

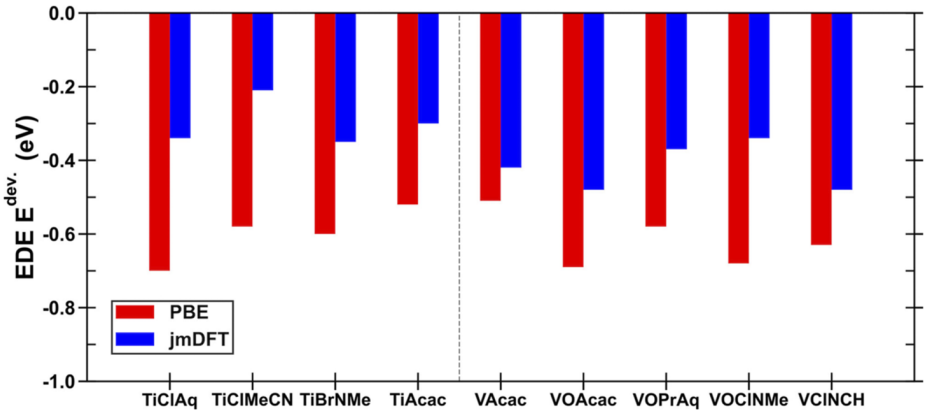

FIG. 2. Energetic delocalization error (EDE) quantified as the maximum deviation, $E^{dev.}$, from linearity (negative values in eV) occurring at the midpoint of the d^0 to d^1 FCL for all Ti and V complexes. $E^{dev.}$ computed using the PBE functional is indicated in red bars while $E^{dev.}$ computed with the standard jmDFT correction using non-empirical U and J on the metal d atomic orbitals is indicated in blue bars. All complexes are annotated using the nomenclature introduced earlier. Ti complexes are to the left of the vertical gray dashed line, and V complexes are to its right.

S4–S5). Still, the EDE reduction is inefficient (<50% for most Ti and V complexes) with standard jmDFT (Fig. 2 and supplementary material, Table S4). This behavior is expected due to the previous observation of inefficiencies in EDE reduction with standard atomic projection DFT+U[84,88] at non-empirical U values.

Despite its success in reducing EDE, a +U correction is known to increase the SCE in all cases because it penalizes all fractional occupations, even the splitting of an electron between degenerate spin-up and spin-down orbitals.[85] The jmDFT approach avoids this by introducing $+J$ and $+J'$ terms that instead favor fractionally occupied spins. We analyze the influence of jmDFT with standard atomic projections on the SCE along the fractional spin line (FSL) of the Ti and V complexes and compare it with the SCE observed with DFT+U alone (Fig. 3 and supplementary material, Fig. S1 and Tables S5–S6). We quantify the SCE as the maximum positive $E^{dev.}$ from exact energetic equivalence (i.e., the energy is unchanged when the electron is alternately spin up or spin down) that occurs at the midpoint of the FSL (Fig. 3). Assuming a constant average curvature along the FSL, we can estimate this deviation using the frontier eigenvalues of the d^1 system alone,[26,86]

$$E^{\text{dev.}} = \frac{\varepsilon_{N+1}^{\text{LUMO}} - \varepsilon_{N+1}^{\text{HOMO}}}{4}. \quad (7)$$

For PBE, the SCE is positive, ranging from 0.2 eV [i.e., for $Ti(acac)_3$] to 0.5 eV [i.e., for $VO(acac)_2$], with comparable values for most complexes (Fig. 3 and supplementary material, Table S6). Standard DFT+U increases this SCE further for all complexes to as large as 1.6 eV [i.e., for $VO(acac)_2$] although the increase is smaller [e.g., 0.4 eV for $Ti(acac)_3$] for other complexes (supplementary material, Table S6). In contrast, applying jmDFT with non-empirical U and J values and standard atomic projectors reduces SCE across most complexes (Fig. 3 and supplementary material, Tables S5–S6). The largest SCE reduction (74%) is observed for a V complex [i.e., $VOCl_2(NH(CH_3)_2)_2$], while for Ti complexes, the SCE reduction is only up to 40% [i.e., $TiBr_3(N(CH_3)_3)_2$]. This behavior is not universal for a given metal as inefficient SCE reduction was also observed in the case of a V complex [i.e., $VCl_4(NCH)_2$] and at its extreme, standard jmDFT showed no effect on $Ti(acac)_3$ (Fig. 3 and supplementary material, Table S6).

Thus, jmDFT holds promise for being one of the few methods that reduces EDE without increasing SCE or computational cost, but we have yet to demonstrate that this elimination occurs at the non-empirical parameter values for TM complexes to the same extent we demonstrated in atoms.[86] In previous work,[88] we observed that inefficiencies in DFT+U EDE elimination could be traced to hybridization in molecular complexes in a manner that made atomic

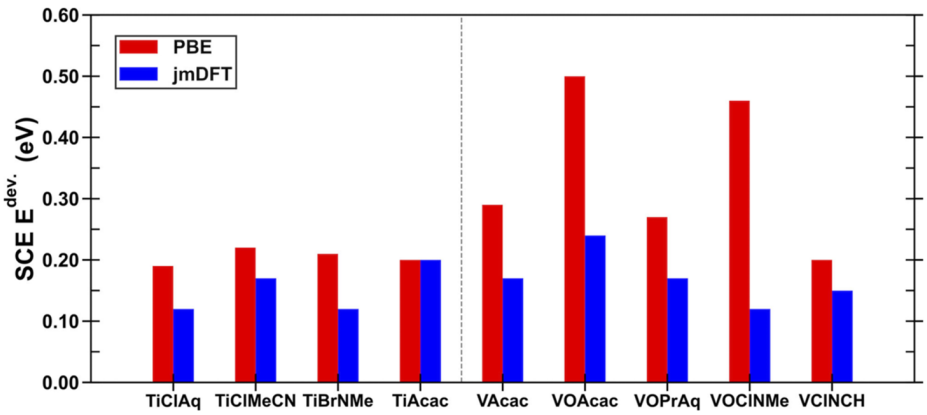

FIG. 3. Static correlation error (SCE) quantified as the maximum deviation, $E^{dev.}$, from energetic equivalence (positive values in eV) occurring at the FSL midpoint for representative Ti and V complexes. $E^{dev.}$ computed using the PBE functional is indicated by red bars, while $E^{dev.}$ computed with the standard jmDFT correction using non-empirical U and J on the metal d atomic orbitals is indicated by blue bars. All complexes are annotated using the nomenclature introduced earlier. Ti complexes are to the left of the vertical gray dashed line, and V complexes are to its right.

projectors unsuitable for obtaining occupations used in DFT+U corrections. We next investigate if apparent inefficiencies in jmDFT SCE elimination similarly result from using atomic projectors.

B. Improving SCE correction efficiency with molecular orbital projectors in jmDFT

In previous work,[84] we attributed the inefficiencies in DFT+U EDE elimination in molecular complexes to the use of metal-centered atomic orbital projectors (AOPs) within DFT+U. Strong metal–ligand hybridization in the frontier orbital to which the fractional electron is added (i.e., along the FCL) made AOPs inefficient for reducing the delocalization error.[84] To determine whether inefficiencies in the elimination of SCE by jmDFT also arise due to the use of metal-centered AOPs, we analyze the hybridization in the frontier orbital along the FSL (Fig. 4 and supplementary material, Tables S7–S15). For a representative Ti complex, Ti(III)(acac)$_3$, the SCE reduction using AOP-based non-empirical jmDFT was negligible relative to the PBE GGA value (see Sec. III A and the supplementary material, Table S6). We indeed find that the contribution from Ti(3*d*) AOs to the HOMO at the FSL midpoint is less than 50% (Fig. 4). The C(2*p*) and O(2*p*) AOs on the ligands contribute comparably to this HOMO, suggesting that metal-centered AOPs alone will be insufficient in describing the fractional spin change along the FSL. Similarly, V complexes also exhibit strong metal–ligand hybridization with their ligand AOs making a significant [e.g., $VCl_4(NCH)_2$, 32%] contribution to the FSL HOMO (supplementary material, Table S15). This highlights that the use of metal-local AOPs will limit SCE reduction efficiency for TM complexes.

Based on previous work,[84,88] the presence of metal–ligand hybridization suggests that the use of molecular orbitals as projectors (MOPs) may lead to higher SCE reduction efficiency. We use the real-space representations of five frontier MOs from the d^1 configuration for each complex as our MOPs (supplementary material, Text S2 and Tables S16–S24). For constructing these MOPs, we select the majority-spin, α, MO containing the single unpaired electron in the d^1 system as well as the next four higher-energy α MOs and the corresponding β MOs from the minority spin (supplementary material, Tables S16–S24).

We quantified the extent to which these MOPs reduce SCE in strongly hybridized complexes (Fig. 5). Because a +J correction with a negative J value is used to reduce SCE within jmDFT,[85,86] we first investigate SCE reduction only using the +J correction,[68,128]

$$E^{DFT+J} = E^{DFT} + \frac{1}{2}\sum_{\sigma} J[\mathrm{Tr}(\mathbf{n_\sigma n_{-\sigma}})]. \tag{8}$$

To a first-order approximation, the PBE fractionality $\mathrm{Tr}[\mathbf{n}_\alpha\mathbf{n}_\beta]$ determines the efficiency of SCE reduction for a given projector choice. If idealized occupations are obtained, the $\mathrm{Tr}[\mathbf{n}_\alpha\mathbf{n}_\beta]$ term should be parabolic with a maximum value of 0.25 e^2 when the electron is split between α and β orbitals (Fig. 5). At odds with this ideal behavior, the Ti(III)(acac)$_3$ AOP fractionalities are nearly constant along the FSL (Fig. 5). Correspondingly, the AOP fractionality deviations (i.e., the difference between the midpoint and a linear admixture of the endpoint values) are significantly smaller (<0.10 e^2) than the atomic limit maximum. In contrast, MOP fractionality variations are parabolic along the FSL with a large fractionality deviation (0.23 e^2) that is close to the atomic limit. This suggests the MOPs should be efficient for reducing SCE in Ti(III)(acac)$_3$.

To quantify differences in efficiency, we compute the linearized sensitivity of the SCE with increasingly negative J values, S_J(SCE) for both AOPs and MOPs (Fig. 6). We indeed observe that MOPs have much higher S_J(SCE) and thus reduce the SCE efficiently

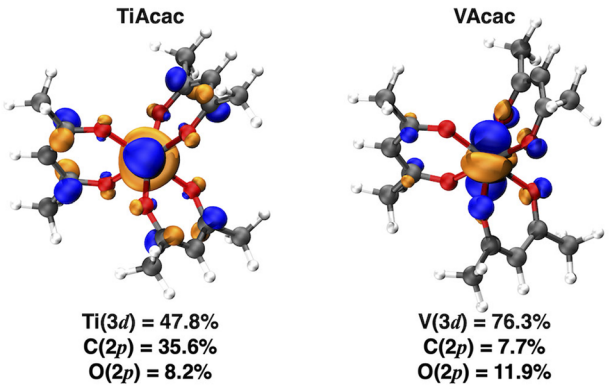

FIG. 4. Density isosurface (isovalue = 0.003 e^-/bohr^3) for the highest occupied molecular orbital (HOMO) of the $(n_\alpha, n_\beta) = (\frac{1}{2}, \frac{1}{2})$ system of Ti(III)(acac)$_3$ (left) and V(IV)(acac)$_3$ (right). Blue denotes the positive wavefunction phase, and orange denotes the negative wavefunction phase. Carbon, oxygen, and hydrogen atoms are shown using gray, red, and white spheres, respectively. Atomic orbital (AO) contributions to the HOMO are annotated for Ti(3*d*), V(3*d*), C(2*p*), and O(2*p*) AOs, where contributions are summed over all atoms of the same type and all angular momenta for each AO.

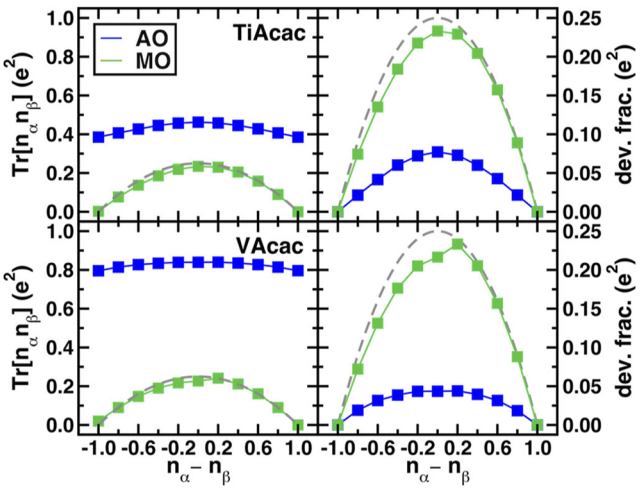

FIG. 5. PBE GGA fractionalities (i.e., $\mathrm{Tr}[\mathbf{n}_\alpha\mathbf{n}_\beta]$ in e^2, left) and deviations from a linear admixture of the integer endpoint values (dev. frac. in e^2, right) for TiAcac [top, Ti(III)(acac)$_3$] and VAcac [bottom, V(IV)(acac)$_3$], where "acac" corresponds to the acetylacetonate ligand, along the fractional spin line. Fractionalities and the deviations were obtained using both atomic orbital (AO) projectors (blue squares) and molecular orbital (MO) projectors obtained from the state with formal d^1 configuration (green squares). Fractionalities and fractionality deviations at the ideal atomic limit are indicated using gray dashed lines.

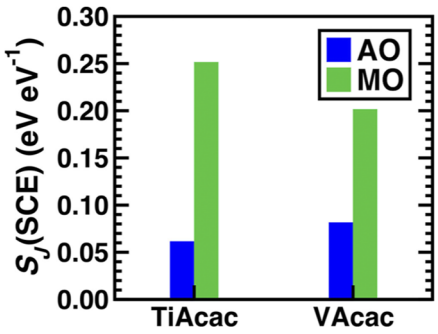

FIG. 6. Linearized sensitivities of static correlation error (SCE) to increasingly negative J values at U = 0 [S_J(SCE), in eV/eV of J] evaluated for TiAcac [i.e., Ti(III)(acac)$_3$] and VAcac [i.e., V(IV)(acac)$_3$], where "acac" corresponds to the acetylacetonate ligand, using AO projectors (blue bars) and MO projectors (green bars).

for Ti(III)(acac)$_3$ (Fig. 6). Other strongly hybridizing complexes [e.g., $VCl_4(NCH)_2$] similarly benefit from the use of MOPs, as is clear from higher MOP fractionality deviations and higher MOP-based SCE reduction efficiencies (supplementary material, Table S15 and Fig. S2).

When hybridization is not the culprit for low efficiency of SCE or EDE reduction, more subtle changes in occupations between electron configurations have also been shown to cause smaller efficiencies than the idealized values.[84,88] V(IV)(acac)$_3$, has a significantly higher (>75%) metal 3d AO contribution to the HOMO at its FSL midpoint than Ti(III)(acac)$_3$ (Fig. 4 and supplementary material, Table S11). However, we observe that its maximum AOP fractionality deviation (0.04 e^2) is not only lower than the atomic limit but lower than that for Ti(III)(acac)$_3$ (0.08 e^2) (Fig. 5). In this case, the use of MOPs also results in higher fractionality deviations and S_J(SCE) values for V(IV)(acac)$_3$ (Fig. 6). MOPs eliminate SCE across a range of hybridization regimes that otherwise limit the suitability of jmDFT with AOPs. We next investigate whether jmDFT with non-empirical U and J terms[85] can robustly eliminate both errors (i.e., the flat-plane error) for all nine Ti and V complexes.

C. Applying molecular jmDFT to transition-metal complexes

The MO DFT+U approach has previously been observed to be more efficient at EDE reduction than the AO-based approach for a range of hybridizations in 3d TM complexes.[88] Taken together with the higher efficiency of the MO DFT+J correction toward SCE reduction, we therefore expect that MO jmDFT will be an ideal framework to simultaneously reduce EDE and SCE. Still, to remain fully non-empirical, we also require that MO-based error reduction efficiencies be close to the theoretically optimal values typically achieved only on model systems.[84,86] We thus investigate the MO-based EDE and SCE reduction efficiencies for all complexes relative to their idealized values[84,86] before analyzing how well this translates to an elimination of both errors within MO jmDFT.

For all nine Ti and V complexes, we computed both the SCE reduction efficiencies using S_J(SCE), as defined earlier, and the EDE reduction efficiency using S_U(EDE) evaluated with increasingly positive U values (Fig. 7). The optimal efficiencies for EDE and SCE reduction on model systems are 0.125 eV/eV of U[84] for S_U(EDE) and 0.25 eV/eV of J[86] for S_J(SCE). As expected, the MO approach reduces errors more efficiently than the AO approach for both EDE and SCE across all Ti and V complexes, achieving close to the idealized limit (Fig. 7). The MO approach achieves universally higher S_J(SCE) values with all at least 80% of the idealized limit (i.e., 0.20 eV/eV or above). The MO-based S_U(EDE) varies more widely with most Ti complexes having values closer to the idealized limit value of 0.125 eV/eV. Some V complexes have lower MO S_U(EDE) values due to shifts in frontier orbital ordering at moderate U values [e.g., V(acac)$_3$, supplementary material, Fig. S3]. Nevertheless, the broadly good sensitivities obtained with the MO approach suggest that MO jmDFT should largely reduce both errors simultaneously in a non-empirical framework.

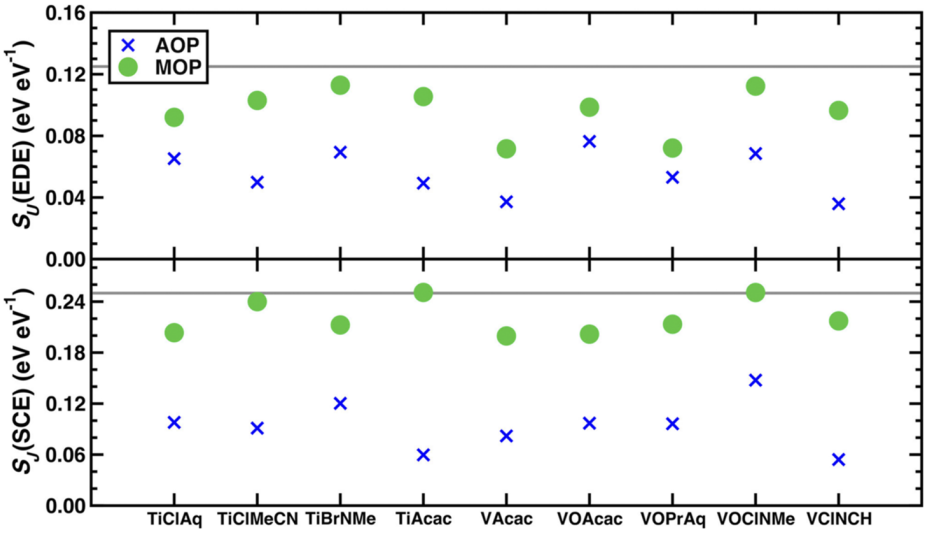

FIG. 7. Linearized sensitivities of the energetic delocalization error (EDE, top) and static correlation error (SCE, bottom) to increasingly positive U values at J = 0 eV [S_U(EDE) in eV per eV of U] and increasingly negative J values at U = 0 eV [S_J(SCE) in eV per eV of J], respectively, for all Ti and V complexes under study. Sensitivities were evaluated using AO projectors (blue crosses) and MO projectors (green circles). Theoretical maximum values of each sensitivity at the atomic limit are indicated by a solid gray line.

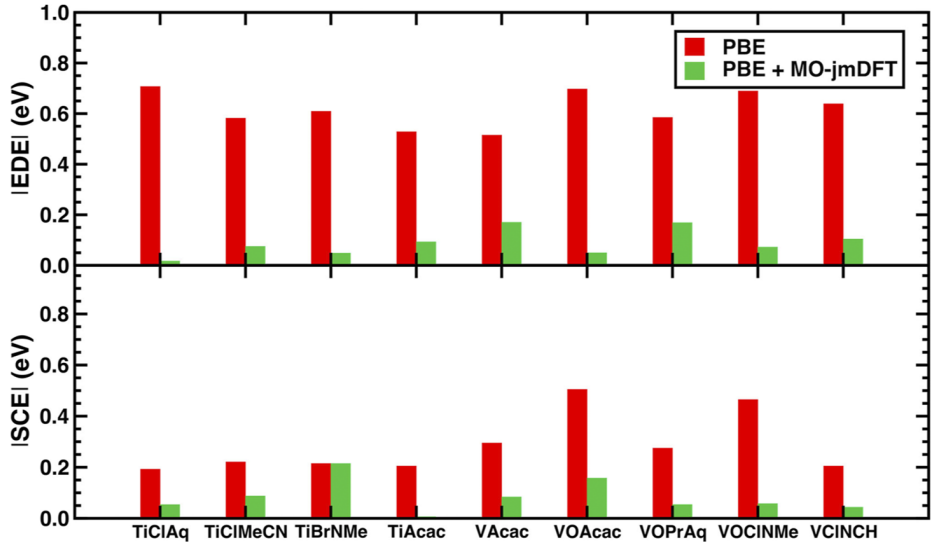

FIG. 8. Energetic delocalization error (EDE, top) quantified as the absolute maximum deviation from linearity (in eV) at the midpoint of the d^0 to d^1 FCL for all Ti and V complexes. (Bottom) Static correlation error (SCE, bottom) quantified as the absolute maximum deviation from energetic invariance (in eV) at the FSL midpoint for all Ti and V complexes. All errors are computed using the PBE functional (red bars) and with the MOP-based jmDFT correction using non-empirical U and J values (green bars).

Finally, we computed EDE and SCE at non-empirical jmDFT values using the MOP approach (Fig. 8). We observe that both errors are largely reduced across most Ti and V complexes. Consistent with the sensitivity analysis, EDEs were virtually eliminated for the Ti complexes with greater than 80% reduction (Figs. 7 and 8). Similarly, EDE reduction for the V complexes was slightly less effective (e.g., VAcac) due to lower MO S_U(EDE) values, but these reductions are still larger than those obtained from the AOP approach (supplementary material, Table S25). The universally higher S_J(SCE) values with the MOP approach indeed translate to a simultaneously large reduction in the SCE. For example, the MOP approach nearly eliminates the SCE for $Ti(acac)_3$ and $VOCl_2(NH(CH_3)_2)_2$ (Fig. 8). For V complexes, SCE reduction with the MOP jmDFT correction is far more consistent than it was with AOPs, generally reducing the SCE by greater than 70% (supplementary material, Table S25). This good performance includes cases where the AOP approach was already observed to be relatively efficient as in $VOCl_2(NH(CH_3)_2)_2$. Similarly, for Ti complexes, SCEs are nearly eliminated using the MOP jmDFT approach except for the case of $TiBr_3(N(CH_3)_3)_2$ due to a change in frontier orbital ordering with J values close to the non-empirical values (supplementary material, Fig. S4). Overall, we observe that MOP-based jmDFT offers an efficient way for recovering exact conditions in nearly all TM complexes within a non-empirical framework at the low cost of semi-local DFT.

A final question is the extent to which eliminating flat-plane errors improves property prediction. As a demonstration of the promise of using both jmDFT within the MOP scheme, we computed the ionization potential of $VO(acac)_2$, a common degradation product of the $V(acac)_3$ redox couple used in redox flow batteries.[129] The experimental ionization potential of this compound obtained with gas-phase UV-photoelectron spectroscopy is 7.36 eV.[130] When we compute the same quantity using the frontier orbital energies (i.e., HOMO) with non-empirical, AOP jmDFT, we obtain a significant underestimate (3.75 eV) of the ionization potential. By applying the non-empirical, MOP scheme within jmDFT, we significantly improve predictions, obtaining a value of 6.34 eV. Similar improvements are obtained with MOP jmDFT on the ionization potential from the total energy difference. For total energy differences, the MOP jmDFT value is a slight overestimate (8.25 eV). Here, the AOP jmDFT scheme is the most inaccurate, underestimating the ionization potential (5.91 eV) even in comparison to the value obtained from PBE total energy differences (6.37 eV). Thus, MOP jmDFT has significant promise in the non-empirical correction of properties that can be expected to be improved when flat-plane errors are eliminated.

IV. CONCLUSIONS

Here, we demonstrated the jmDFT method, an approach to recovering exact conditions at semi-local DFT cost, on the electronic structure of transition-metal complexes. We analyzed the errors of the PBE functional along the fractional spin line of a set of Ti and V d^1 complexes as well as the fractional charge line between d^0 and d^1 electron configurations. We rationalized inefficiencies observed for standard (i.e., AOP) jmDFT by noting hybridization in the relevant frontier orbitals. This led to lower-than-expected fractional occupations detected by the AO projections along the FSL, an observation we had previously only made along the FCL. To overcome these limitations, we introduced a procedure for computing an MOP basis for jmDFT. We demonstrated this single set of d^1 MOPs to be suitable for nearly eliminating all energetic delocalization and static correlation errors along the FCL and FSL, respectively. In most cases, MOP jmDFT outperformed AOP jmDFT, and analysis of frontier orbital energies can be used to rationalize where the MOP procedure will fail. Furthermore, unlike DFT+U, jmDFT never improved the energetic delocalization error at the cost of worsening the static correlation error. Thus, we expect that MOP jmDFT should consistently provide an improvement over both DFT+U and AOP jmDFT. The drawback of this approach is that the MOPs must be generated for each system. The determination of the parameters is non-empirical and obtained from frontier orbital

energies at the PBE level and so, like any flat-plane-based tuning approach, will be system-specific but relatively low cost to obtain. One consideration is that the parameters themselves will potentially vary along a reaction coordinate in which case a variable-parameter approach such as a generalization of DFT+$U(\mathbf{R})$[131] would be necessary. Overall, we expect this non-empirical approach and systematic construction of jmDFT MOPs to be broadly useful in high-throughput screening in transition-metal catalysis where barrier heights and reaction energetics can be expected to be sensitive to both delocalization and static correlation errors.

SUPPLEMENTARY MATERIAL

See the supplementary material for the extraction of transition-metal complexes with d^1 configuration from the literature; CSD refcodes and chemical formulas of the final nine complexes; list of pseudopotentials used; construction of real-space molecular orbitals; a representative exact flat-plane construction; energetic delocalization error (EDE) at the PBE and atomic jmDFT levels; non-empirical values of U and J for all nine Ti and V complexes; static correlation error (SCE) at the PBE, PBE+U and atomic jmDFT levels; atomic orbital character of frontier spin-up MOs for the FSL of TiClAq; atomic orbital character of frontier spin-up MOs for the FSL of TiClMeCN; atomic orbital character of frontier spin-up MOs for the FSL of TiBrNMe; atomic orbital character of frontier spin-up MOs for the FSL of TiAcac; atomic orbital character of frontier spin-up MOs for the FSL of VAcac; atomic orbital character of frontier spin-up MOs for the FSL of VOAcac; atomic orbital character of frontier spin-up MOs for the FSL of VOPrAq; atomic orbital character of frontier spin-up MOs for the FSL of VOClNMe; atomic orbital character of frontier spin-up MOs for the FSL of VClNCH; atomic orbital character of the projector MOs of TiClAq; atomic orbital character of the projector MOs of TiClMeCN; atomic orbital character of the projector MOs of TiBrNMe; atomic orbital character of the projector MOs of TiAcac; atomic orbital character of the projector MOs of VAcac; atomic orbital character of the projector MOs of VOAcac; atomic orbital character of the projector MOs of VOPrAq; atomic orbital character of the projector MOs of VOClNMe; atomic orbital character of the projector MOs of VClNCH; FSL fractionality analysis and SCE reduction efficiencies for VClNCH; frontier eigenvalue variations for VAcac with U using MO projectors; EDE and SCE values for PBE, atomic jmDFT and molecular jmDFT; frontier eigenvalue variations for TiBrNMe with J using MO projectors (PDF); and structures of all molecules studied in this work (ZIP).

ACKNOWLEDGMENTS

This work was primarily supported by the U.S. Department of Energy under Grant No. DE-SC0018096. Workflows used in this work were supported under Office of Naval Research Grant Nos. N00014-18-1-2434 and N00014-20-1-2150 (C.D. and M.G.T.) and National Science Foundation Grant No. CBET-1846426 (A.N.). This work was also partially supported by a National Science Foundation Graduate Research Fellowship under Grant No. 1122374 (to A.N.). H.J.K. holds a Career Award at the Scientific Interface from the Burroughs Wellcome Fund, an AAAS Marion Milligan Mason Award, and an Alfred P. Sloan award in Chemistry, which supported this work. This work made use of the Extreme Science and Engineering Discovery Environment (XSEDE), which is supported by National Science Foundation Grant No. ACI-1548562. The authors thank Adam H. Steeves for providing a critical reading of the manuscript.

AUTHOR DECLARATIONS

Conflict of Interest

The authors have no conflicts to disclose.

DATA AVAILABILITY

The data that support the findings of this study are available within the article and its supplementary material.

REFERENCES

[1] A. D. Becke, "Perspective: Fifty years of density-functional theory in chemical physics," J. Chem. Phys. **140**, 18A301 (2014).
[2] K. Burke, "Perspective on density functional theory," J. Chem. Phys. **136**, 150901 (2012).
[3] H. S. Yu, S. L. Li, and D. G. Truhlar, "Perspective: Kohn-Sham density functional theory descending a staircase," J. Chem. Phys. **145**, 130901 (2016).
[4] W. Kohn, "Nobel lecture: Electronic structure of matter-wave functions and density functionals," Rev. Mod. Phys. **71**, 1253–1266 (1999).
[5] A. Jain, S. P. Ong, G. Hautier, W. Chen, W. D. Richards, S. Dacek, S. Cholia, D. Gunter, D. Skinner, G. Ceder *et al.*, "Commentary: The materials project: A materials genome approach to accelerating materials innovation," APL Mater. **1**, 011002 (2013).
[6] J. K. Norskov and T. Bligaard, "The catalyst genome," Angew. Chem., Int. Ed. **52**, 776–777 (2013).
[7] J. C. Slater, *The Self-Consistent Field for Molecules and Solids: Quantum Theory of Molecules and Solids* (McGraw-Hill Book Company, 1974).
[8] S. H. Vosko, L. Wilk, and M. Nusair, "Accurate spin-dependent electron liquid correlation energies for local spin-density calculations—A critical analysis," Can. J. Phys. **58**, 1200–1211 (1980).
[9] A. D. Becke, "Density-functional exchange-energy approximation with correct asymptotic-behavior," Phys. Rev. A **38**, 3098–3100 (1988).
[10] C. Lee, W. Yang, and R. G. Parr, "Development of the Colle-Salvetti correlation-energy formula into a functional of the electron-density," Phys. Rev. B **37**, 785–789 (1988).
[11] J. P. Perdew, K. Burke, and M. Ernzerhof, "Generalized gradient approximation made simple," Phys. Rev. Lett. **77**, 3865–3868 (1996).
[12] P. Mori-Sánchez, A. J. Cohen, and W. Yang, "Many-electron self-interaction error in approximate density functionals," J. Chem. Phys. **125**, 201102 (2006).
[13] A. Ruzsinszky, J. P. Perdew, G. I. Csonka, O. A. Vydrov, and G. E. Scuseria, "Density functionals that are one- and two- are not always many-electron self-interaction-free, as shown for H_2^+, He_2^+, LiH^+, and Ne_2^+," J. Chem. Phys. **126**, 104102 (2007).
[14] R. Haunschild, T. M. Henderson, C. A. Jiménez-Hoyos, and G. E. Scuseria, "Many-electron self-interaction and spin polarization errors in local hybrid density functionals," J. Chem. Phys. **133**, 134116 (2010).
[15] A. J. Cohen, P. Mori-Saánchez, and W. Yang, "Insights into current limitations of density functional theory," Science **321**, 792–794 (2008).
[16] T. Schmidt and S. Kümmel, "One- and many-electron self-interaction error in local and global hybrid functionals," Phys. Rev. B **93**, 165120 (2016).
[17] J. P. Perdew, R. G. Parr, M. Levy, and J. L. Balduz, "Density-functional theory for fractional particle number—Derivative discontinuities of the energy," Phys. Rev. Lett. **49**, 1691–1694 (1982).

[18]T. Stein, J. Autschbach, N. Govind, L. Kronik, and R. Baer, "Curvature and frontier orbital energies in density functional theory," J. Phys. Chem. Lett. **3**, 3740–3744 (2012).
[19]W. Yang, Y. Zhang, and P. W. Ayers, "Degenerate ground states and a fractional number of electrons in density and reduced density matrix functional theory," Phys. Rev. Lett. **84**, 5172–5175 (2000).
[20]J. P. Perdew and M. Levy, "Physical content of the exact Kohn-Sham orbital energies—Band-gaps and derivative discontinuities," Phys. Rev. Lett. **51**, 1884–1887 (1983).
[21]L. J. Sham and M. Schlüter, "Density-functional theory of the energy-gap," Phys. Rev. Lett. **51**, 1888–1891 (1983).
[22]E. Sagvolden and J. P. Perdew, "Discontinuity of the exchange-correlation potential: Support for assumptions used to find it," Phys. Rev. A **77**, 012517 (2008).
[23]P. Mori-Sánchez and A. J. Cohen, "The derivative discontinuity of the exchange-correlation functional," Phys. Chem. Chem. Phys. **16**, 14378–14387 (2014).
[24]M. C. Kim, E. Sim, and K. Burke, "Understanding and reducing errors in density functional calculations," Phys. Rev. Lett. **111**, 073003 (2013).
[25]X. Zheng, M. Liu, E. R. Johnson, J. Contreras-García, and W. Yang, "Delocalization error of density-functional approximations: A distinct manifestation in hydrogen molecular chains," J. Chem. Phys. **137**, 214106 (2012).
[26]E. R. Johnson, A. Otero-De-La-Roza, and S. G. Dale, "Extreme density-driven delocalization error for a model solvated-electron system," J. Chem. Phys. **139**, 184116 (2013).
[27]P. Mori-Sánchez, A. J. Cohen, and W. Yang, "Localization and delocalization errors in density functional theory and implications for band-gap prediction," Phys. Rev. Lett. **100**, 146401 (2008).
[28]F. Liu and H. J. Kulik, "Impact of approximate DFT density delocalization error on potential energy surfaces in transition metal chemistry," J. Chem. Theory Comput. **16**, 264–277 (2020).
[29]T. J. Duignan and J. Autschbach, "Impact of the Kohn-Sham delocalization error on the 4f shell localization and population in lanthanide complexes," J. Chem. Theory Comput. **12**, 3109–3121 (2016).
[30]M. G. Medvedev, I. S. Bushmarinov, J. Sun, J. P. Perdew, and K. A. Lyssenko, "Density functional theory is straying from the path toward the exact functional," Science **355**, 49–52 (2017).
[31]B. Pritchard and J. Autschbach, "Theoretical investigation of paramagnetic NMR shifts in transition metal acetylacetonato complexes: Analysis of signs, magnitudes, and the role of the covalency of ligand-metal bonding," Inorg. Chem. **51**, 8340–8351 (2012).
[32]B. G. Janesko, "Reducing density-driven error without exact exchange," Phys. Chem. Chem. Phys. **19**, 4793–4801 (2017).
[33]D. J. Tozer and F. De Proft, "Computation of the hardness and the problem of negative electron affinities in density functional theory," J. Phys. Chem. A **109**, 8923–8929 (2005).
[34]A. M. Teale, F. De Proft, and D. J. Tozer, "Orbital energies and negative electron affinities from density functional theory: Insight from the integer discontinuity," J. Chem. Phys. **129**, 044110 (2008).
[35]M. J. G. Peach, A. M. Teale, T. Helgaker, and D. J. Tozer, "Fractional electron loss in approximate DFT and Hartree-Fock theory," J. Chem. Theory Comput. **11**, 5262–5268 (2015).
[36]L. Kronik and S. Kümmel, "Piecewise linearity, freedom from self-interaction, and a coulomb asymptotic potential: Three related yet inequivalent properties of the exact density functional," Phys. Chem. Chem. Phys. **22**, 16467–16481 (2020).
[37]A. J. Cohen, P. Mori-Sánchez, and W. Yang, "Fractional charge perspective on the band gap in density-functional theory," Phys. Rev. B **77**, 115123 (2008).
[38]P. Huang and E. A. Carter, "Advances in correlated electronic structure methods for solids, surfaces, and nanostructures," Annu. Rev. Phys. Chem. **59**, 261–290 (2008).
[39]H. J. Kulik, M. Cococcioni, D. A. Scherlis, and N. Marzari, "Density functional theory in transition-metal chemistry: A self-consistent Hubbard U approach," Phys. Rev. Lett. **97**, 103001 (2006).
[40]G. Ganzenmüller, N. Berkaïne, A. Fouqueau, M. E. Casida, and M. Reiher, "Comparison of density functionals for differences between the high-($^5T_{2g}$) and low-($^1A_{1g}$) spin states of iron(II) compounds. IV. Results for the ferrous complexes [Fe(L)('NHS$_4$')]," J. Chem. Phys. **122**, 234321 (2005).
[41]A. Droghetti, D. Alfè, and S. Sanvito, "Assessment of density functional theory for iron(II) molecules across the spin-crossover transition," J. Chem. Phys. **137**, 124303 (2012).
[42]E. I. Ioannidis and H. J. Kulik, "Towards quantifying the role of exact exchange in predictions of transition metal complex properties," J. Chem. Phys. **143**, 034104 (2015).
[43]S. R. Mortensen and K. P. Kepp, "Spin propensities of octahedral complexes from density functional theory," J. Phys. Chem. A **119**, 4041–4050 (2015).
[44]E. I. Ioannidis and H. J. Kulik, "Ligand-field-dependent behavior of meta-gga exchange in transition-metal complex spin-state ordering," J. Phys. Chem. A **121**, 874–884 (2017).
[45]G. Prokopiou and L. Kronik, "Spin-state energetics of Fe complexes from an optimally tuned range-separated hybrid functional," Chem. Eur. J. **24**, 5173–5182 (2018).
[46]F. Liu, T. Yang, J. Yang, E. Xu, A. Bajaj, and H. J. Kulik, "Bridging the homogeneous-heterogeneous divide: Modeling spin for reactivity in single atom catalysis," Front. Chem. **7**, 219 (2019).
[47]M. G. Taylor, T. Yang, S. Lin, A. Nandy, J. P. Janet, C. Duan, and H. J. Kulik, "Seeing is believing: Experimental spin states from machine learning model structure predictions," J. Phys. Chem. A **124**, 3286–3299 (2020).
[48]C. Zhang, T. A. Pham, F. Gygi, and G. Galli, "Communication: Electronic structure of the solvated chloride anion from first principles molecular dynamics," J. Chem. Phys. **138**, 181102 (2013).
[49]T. A. Pham, M. Govoni, R. Seidel, Se. Bradforth, E. Schwegler, and G. Galli, "Electronic structure of aqueous solutions: Bridging the gap between theory and experiments," Sci. Adv. **3**, e1603210 (2017).
[50]N. Marom, O. Hod, G. E. Scuseria, and L. Kronik, "Electronic structure of copper phthalocyanine: A comparative density functional theory study," J. Chem. Phys. **128**, 164107 (2008).
[51]J. Autschbach and M. Srebro, "Delocalization error and "functional tuning" in Kohn-Sham calculations of molecular properties," Acc. Chem. Res. **47**, 2592–2602 (2014).
[52]S. Kümmel and L. Kronik, "Orbital-dependent density functionals: Theory and applications," Rev. Mod. Phys. **80**, 3–60 (2008).
[53]B. G. Janesko, "Rung 3.5 density functionals," J. Chem. Phys. **133**, 104103 (2010).
[54]T. Stein, H. Eisenberg, L. Kronik, and R. Baer, "Fundamental gaps in finite systems from eigenvalues of a generalized Kohn-Sham method," Phys. Rev. Lett. **105**, 266802 (2010).
[55]S. Refaely-Abramson, R. Baer, and L. Kronik, "Fundamental and excitation gaps in molecules of relevance for organic photovoltaics from an optimally tuned range-separated hybrid functional," Phys. Rev. B **84**, 075144 (2011).
[56]O. A. Vydrov and G. E. Scuseria, "Assessment of a long-range corrected hybrid functional," J. Chem. Phys. **125**, 234109 (2006).
[57]A. J. Cohen, P. Mori-Sánchez, and W. Yang, "Development of exchange-correlation functionals with minimal many-electron self-interaction error," J. Chem. Phys. **126**, 191109 (2007).
[58]R. Baer and D. Neuhauser, "Density functional theory with correct long-range asymptotic behavior," Phys. Rev. Lett. **94**, 043002 (2005).
[59]T. M. Henderson, B. G. Janesko, and G. E. Scuseria, "Range separation and local hybridization in density functional theory," J. Phys. Chem. A **112**, 12530–12542 (2008).
[60]B. G. Janesko, T. M. Henderson, and G. E. Scuseria, "Screened hybrid density functionals for solid-state chemistry and physics," Phys. Chem. Chem. Phys. **11**, 443–454 (2009).
[61]M. A. Rohrdanz, K. M. Martins, and J. M. Herbert, "A long-range-corrected density functional that performs well for both ground-state properties and time-dependent density functional theory excitation energies, including charge-transfer excited states," J. Chem. Phys. **130**, 054112 (2009).
[62]A. V. Krukau, O. A. Vydrov, A. F. Izmaylov, and G. E. Scuseria, "Influence of the exchange screening parameter on the performance of screened hybrid functionals," J. Chem. Phys. **125**, 224106 (2006).
[63]T. Yanai, D. P. Tew, and N. C. Handy, "A new hybrid exchange-correlation functional using the coulomb-attenuating method (CAM-B3LYP)," Chem. Phys. Lett. **393**, 51–57 (2004).

[64]J. H. Skone, M. Govoni, and G. Galli, "Self-consistent hybrid functional for condensed systems," Phys. Rev. B **89**, 195112 (2014).
[65]J. H. Skone, M. Govoni, and G. Galli, "Nonempirical range-separated hybrid functionals for solids and molecules," Phys. Rev. B **93**, 235106 (2016).
[66]M. Srebro and J. Autschbach, "Does a molecule-specific density functional give an accurate electron density? The challenging case of the CuCl electric field gradient," J. Phys. Chem. Lett. **3**, 576–581 (2012).
[67]V. I. Anisimov, J. Zaanen, and O. K. Andersen, "Band theory and Mott insulators: Hubbard U instead of Stoner I," Phys. Rev. B **44**, 943 (1991).
[68]A. I. Liechtenstein, V. I. Anisimov, and J. Zaanen, "Density-functional theory and strong-interactions—Orbital ordering in Mott-Hubbard insulators," Phys. Rev. B **52**, R5467–R5470 (1995).
[69]S. L. Dudarev, G. A. Botton, S. Y. Savrasov, C. J. Humphreys, and A. P. Sutton, "Electron-energy-loss spectra and the structural stability of nickel oxide: An LSDA+U study," Phys. Rev. B **57**, 1505–1509 (1998).
[70]H. J. Kulik, "Perspective: Treating electron over-delocalization with the DFT plus U method," J. Chem. Phys. **142**, 240901 (2015).
[71]M. Cococcioni and S. De Gironcoli, "Linear response approach to the calculation of the effective interaction parameters in the LDA+ U method," Phys. Rev. B **71**, 035105 (2005).
[72]P. Liao and E. A. Carter, "Testing variations of the GW approximation on strongly correlated transition metal oxides: Hematite (α-Fe_2O_3) as a benchmark," Phys. Chem. Chem. Phys. **13**, 15189–15199 (2011).
[73]M. C. Toroker, D. K. Kanan, N. Alidoust, L. Y. Isseroff, P. Liao, and E. A. Carter, "First principles scheme to evaluate band edge positions in potential transition metal oxide photocatalysts and photoelectrodes," Phys. Chem. Chem. Phys. **13**, 16644–16654 (2011).
[74]B. Brena, C. Puglia, M. de Simone, M. Coreno, K. Tarafder, V. Feyer, R. Banerjee, E. Göthelid, B. Sanyal, P. M. Oppeneer *et al.*, "Valence-band electronic structure of iron phthalocyanine: An experimental and theoretical photoelectron spectroscopy study," J. Chem. Phys. **134**, 074312 (2011).
[75]D. Klar, B. Brena, H. C. Herper, S. Bhandary, C. Weis, B. Krumme, C. Schmitz-Antoniak, B. Sanyal, O. Eriksson, and H. Wende, "Oxygen-tuned magnetic coupling of Fe-phthalocyanine molecules to ferromagnetic Co films," Phys. Rev. B **88**, 224424 (2013).
[76]I. E. Brumboiu, S. Haldar, J. Lüder, O. Eriksson, H. C. Herper, B. Brena, and B. Sanyal, "Ligand effects on the linear response hubbard U: The case of transition metal phthalocyanines," J. Phys. Chem. A **123**, 3214–3222 (2019).
[77]U. G. E. Perera, H. J. Kulik, V. Iancu, L. G. G. V. Dias da Silva, S. E. Ulloa, N. Marzari, and S.-W. Hla, "Spatially extended Kondo state in magnetic molecules induced by interfacial charge transfer," Phys. Rev. Lett. **105**, 106601 (2010).
[78]S. Lebegue, S. Pillet, and J. G. Angyan, "Modeling spin-crossover compounds by periodic DFT+U approach," Phys. Rev. B **78**, 024433 (2008).
[79]J. Chen, A. J. Millis, and C. A. Marianetti, "Density functional plus dynamical mean-field theory of the spin-crossover molecule $Fe(phen)_2(NCS)_2$," Phys. Rev. B **91**, 241111 (2015).
[80]S. Vela, M. Fumanal, J. Ribas-Arino, and V. Robert, "Towards an accurate and computationally-efficient modelling of Fe(II)-Based spin crossover materials," Phys. Chem. Chem. Phys. **17**, 16306–16314 (2015).
[81]E. B. Linscott, D. J. Cole, M. C. Payne, and D. D. O'Regan, "Role of spin in the calculation of Hubbard U and Hund's J parameters from first principles," Phys. Rev. B **98**, 235157 (2018).
[82]M. Ohlrich and B. J. Powell, "Fast, accurate enthalpy differences in spin crossover crystals from DFT plus," U. J. Chem. Phys. **153**, 104107 (2020).
[83]L. A. Mariano, B. Vlaisavljevich, and R. Poloni, "Biased spin-state energetics of Fe(II) molecular complexes within density-functional theory and the linear-response Hubbard U correction," J. Chem. Theory Comput. **16**, 6755–6762 (2020).
[84]Q. Zhao, E. I. Ioannidis, and H. J. Kulik, "Global and local curvature in density functional theory," J. Chem. Phys. **145**, 054109 (2016).
[85]A. Bajaj, J. P. Janet, and H. J. Kulik, "Communication: Recovering the flat-plane condition in electronic structure theory at semi-local DFT cost," J. Chem. Phys. **147**, 191101 (2017).
[86]A. Bajaj, F. Liu, and H. J. Kulik, "Non-empirical, low-cost recovery of exact conditions with model-Hamiltonian inspired expressions in jmDFT," J. Chem. Phys. **150**, 154115 (2019).
[87]V. I. Anisimov, F. Aryasetiawan, and A. I. Lichtenstein, "First-principles calculations of the electronic structure and spectra of strongly correlated systems: The LDA+ U method," J. Phys.: Condens. Matter **9**, 767 (1997).
[88]A. Bajaj and H. J. Kulik, "Molecular DFT plus U: A transferable, low-cost approach to eliminate delocalization error," J. Phys. Chem. Lett. **12**, 3633–3640 (2021).
[89]K. Yu and E. A. Carter, "Communication: Comparing *ab initio* methods of obtaining effective U parameters for closed-shell materials," J. Chem. Phys. **140**, 121105 (2014).
[90]A. Bajaj and H. J. Kulik, "Eliminating delocalization error to improve heterogeneous catalysis predictions with molecular DFT+U" J. Chem. Theory Comput. **18**, 1142–1155 (2022).
[91]D. Shin, N. Tancogne-Dejean, J. Zhang, M. S. Okyay, A. Rubio, and N. Park, "Identification of the mott insulating charge density wave state in 1T – Ta S_2," Phys. Rev. Lett. **126**, 196406 (2021).
[92]T. Z. H. Gani and H. J. Kulik, "Unifying exchange sensitivity in transition-metal spin-state ordering and catalysis through bond valence metrics," J. Chem. Theory Comput. **13**, 5443–5457 (2017).
[93]A. Mahler, B. G. Janesko, S. Moncho, and E. N. Brothers, "When Hartree-Fock exchange admixture lowers DFT-predicted barrier heights: Natural bond orbital analyses and implications for catalysis," J. Chem. Phys. **148**, 244106 (2018).
[94]M. Modrzejewski, G. Chalasinski, and M. M. Szczesniak, "Assessment of newest meta-GGA hybrids for late transition metal reactivity: Fractional charge and fractional spin perspective," J. Phys. Chem. C **123**, 8047–8056 (2019).
[95]J. Paier, M. Marsman, and G. Kresse, "Why does the B3LYP hybrid functional fail for metals?," J. Chem. Phys. **127**, 024103 (2007).
[96]T. Ko$\acute{}$rzdo$\acute{}$rfer and J.-L. Bredas, "Organic electronic materials: Recent advances in the DFT description of the ground and excited states using tuned range-separated hybrid functionals," Acc. Chem. Res. **47**, 3284–3291 (2014).
[97]S. Kirklin, J. E. Saal, B. Meredig, A. Thompson, J. W. Doak, M. Aykol, S. Rühl, and C. Wolverton, "The open quantum materials database (OQMD): Assessing the accuracy of DFT formation energies," npj Comput. Mater. **1**, 1–15 (2015).
[98]J. Kirkpatrick, B. McMorrow, D. H. P. Turban, A. L. Gaunt, J. S. Spencer, A. G. D. G. Matthews, A. Obika, L. Thiry, M. Fortunato, D. Pfau *et al.*, "Pushing the frontiers of density functionals by solving the fractional electron problem," Science **374**, 1385–1389 (2021).
[99]N. Q. Su, A. Mahler, and W. Yang, "Preserving symmetry and degeneracy in the localized orbital scaling correction approach," J. Phys. Chem. Lett. **11**, 1528–1535 (2020).
[100]C. Li, X. Zheng, N. Q. Su, and W. Yang, "Localized orbital scaling correction for systematic elimination of delocalization error in density functional approximations," Natl. Sci. Rev. **5**, 203–215 (2017).
[101]P. Mori-Sanchez, A. J. Cohen, and W. T. Yang, "Discontinuous nature of the exchange-correlation functional in strongly correlated systems," Phys. Rev. Lett. **102** (2009).
[102]C. R. Groom, I. J. Bruno, M. P. Lightfoot, and S. C. Ward, "The Cambridge structural Database," Acta Crystallogr., Sect. B: Struct. Crystallogr. Cryst. Chem. **72**, 171–179 (2016).
[103]I. S. Ufimtsev and T. J. Martinez, "Quantum chemistry on graphical processing units. 3. Analytical energy gradients, geometry optimization, and first principles molecular dynamics," J. Chem. Theory Comput. **5**, 2619–2628 (2009).
[104]M. Ernzerhof and G. E. Scuseria, "Assessment of the perdew-burke-ernzerhof exchange-correlation functional," J. Chem. Phys. **110**, 5029–5036 (1999).
[105]C. Adamo and V. Barone, "Toward reliable density functional methods without adjustable parameters: The Pbe0 model," J. Chem. Phys. **110**, 6158–6170 (1999).
[106]P. J. Hay and W. R. Wadt, "Abinitio effective core potentials for molecular calculations - potentials for the transition-metal atoms Sc to Hg," J. Chem. Phys. **82**, 270–283 (1985).
[107]W. R. Wadt and P. J. Hay, "Abinitio effective core potentials for molecular calculations - potentials for main group elements Na to Bi," J. Chem. Phys. **82**, 284–298 (1985).
[108]R. Ditchfield, W. J. Hehre, and J. A. Pople, "Self-consistent molecular-orbital methods .9. Extended Gaussian-type basis for molecular-orbital studies of organic molecules," J. Chem. Phys. **54**, 724-+ (1971).

[109]L.-P. Wang and C. Song, "Geometry optimization made simple with translation and rotation coordinates," J. Chem. Phys. **144**, 214108 (2016).
[110]C. G. Broyden, "The convergence of a class of double-rank minimization algorithms 1. General considerations," IMA J. Appl. Math. **6**, 76–90 (1970).
[111]C. G. Broyden, "The convergence of a class of double-rank minimization algorithms: 2. The new algorithm," IMA J. Appl. Math. **6**, 222–231 (1970).
[112]R. Fletcher, "New approach to variable metric algorithms," Comput. J. **13**, 317 (1970).
[113]D. Goldfarb, "A family of variable-metric methods derived by variational means," Math. Comput. **24**, 23 (1970).
[114]D. F. Shanno, "Conditioning of quasi-Newton methods for function minimization," Math. Comput. **24**, 647 (1970).
[115]D. C. Liu and J. Nocedal, "On the limited memory bfgs method for large-scale optimization," Math. Program. **45**, 503–528 (1989).
[116]A. W. Lange and J. M. Herbert, "A smooth, nonsingular, and faithful discretization scheme for polarizable continuum models: The switching/Gaussian approach," J. Chem. Phys. **133**, 244111 (2010).
[117]D. M. York and M. Karplus, "A smooth solvation potential based on the conductor-like screening model," J. Phys. Chem. A **103**, 11060–11079 (1999).
[118]F. Liu, N. Luehr, H. J. Kulik, and T. J. Martínez, "Quantum chemistry for solvated molecules on graphical processing units using polarizable continuum models," J. Chem. Theory Comput. **11**, 3131–3144 (2015).
[119]F. Liu, D. M. Sanchez, H. J. Kulik, and T. J. Martínez, "Exploiting graphical processing units to enable Quantum chemistry calculation of large solvated molecules with conductor-like polarizable continuum models," Int. J. Quantum Chem. **119**, e25760 (2019).
[120]A. Bondi, "Van der Waals volumes and radii," J. Phys. Chem. **68**, 441–451 (1964).
[121]P. Giannozzi, S. Baroni, N. Bonini, M. Calandra, R. Car, C. Cavazzoni, D. Ceresoli, G. L. Chiarotti, M. Cococcioni, I. Dabo *et al.*, "Quantum espresso: A modular and open-source software project for quantum simulations of materials," J. Phys.: Condens. Matter **21**, 395502 (2009).
[122]D. Vanderbilt, "Soft self-consistent pseudopotentials in a generalized eigenvalue formalism," Phys. Rev. B **41**, 7892–7895 (1990).
[123]A. M. Rappe, K. M. Rabe, E. Kaxiras, and J. D. Joannopoulos, "Optimized pseudopotentials," Phys. Rev. B **41**, 1227–1230 (1990).
[124]G. J. Martyna and M. E. Tuckerman, "A reciprocal space based method for treating long range interactions in *ab initio* and force-field-based calculations in clusters," J. Chem. Phys. **110**, 2810–2821 (1999).
[125]N. Marzari, A. A. Mostofi, J. R. Yates, I. Souza, and D. Vanderbilt, "Maximally localized wannier functions: Theory and applications," Rev. Mod. Phys. **84**, 1419–1475 (2012).
[126]W. Humphrey, A. Dalke, and K. Schulten, "VMD: Visual molecular dynamics," J. Mol. Graph. Model. **14**, 33–38 (1996).
[127]K. Momma and F. Izumi, "Vesta 3 for three-dimensional visualization of crystal, volumetric and morphology data," J. Appl. Crystallogr. **44**, 1272–1276 (2011).
[128]B. Himmetoglu, R. M. Wentzcovitch, and M. Cococcioni, "First-principles study of electronic and structural properties of cuo," Phys. Rev. B **84**, 115108 (2011).
[129]A. A. Shinkle, A. E. S. Sleightholme, L. D. Griffith, L. T. Thompson, and C. W. Monroe, "Degradation mechanisms in the non-aqueous vanadium acetylacetonate redox flow battery," J. Power Sources **206**, 490–496 (2012).
[130]N. E. Gruhn, L. J. Michelsen, and B. L. Westcott, "Photoelectron spectroscopy of Bis(2,4-Pentanedione)−Oxovanadium(IV) [$VO(acac)_2$] and derivatives: Substituent effects on the 2,4-pentanedione donor," Inorg. Chem. **41**, 5907–5911 (2002).
[131]H. J. Kulik and N. Marzari, "Accurate potential energy surfaces with a DFT + U(R) approach," J. Chem. Phys. **135**, 194105 (2011).